Some characteristics of the fluid dynamics in nonlinear wave train.

Y.-M. Scolan
ENSTA-Bretagne, IRDL UMR 6027 (France)
yves-marie.scolan@ensta-bretagne.fr

Highlights

- linear and nonlinear wave train,
- spatial/temporal variations of the pressure field and its spatial derivatives,
- collinearity of the pressure gradient and one eigenvector of the pressure Hessian matrix.

The present abstract is concerned with two dimensional wave trains that propagate in a domain over a flat bottom. In the light of recent analyses of the temporal and spatial variations of the pressure field beneath the free surface (see [1] and [2]), we examine what information is available along the lines defined by the collinearity of the pressure gradient and one of the two eigenvectors of the pressure Hessian matrix. It is shown that these two vectors are collinear along a line that always intersects the free surface; it is called the backbone line. Several backbone lines can be identified in the fluid domain. They are always attached to the crests of a wave train. So far we have been mainly interested in the backbone line associated to the main crest, that can possibly break. Here we extend our analysis to the entire wave train and we start from the linear case.

As a first step the simple linear case with monochromatic wave is investigated. It is described in a cartesian coordinate system (x, y). The wave has an amplitude A, wave number k, and it propagates along the positive x axis over a constant water depth h. Given the velocity potential ϕ that describes this Airy wave, the pressure gradient follows from the linearized Euler equation projected on a Cartesian normalized vectors $(\vec{x}, \vec{y})$, yielding the components $p_{,x} = -\rho\phi_{,xt}$ and $p_{,y} = -\rho\phi_{,yt} - \rho g$ (the fluid density is ρ and the acceleration of gravity is g). The elements of pressure Hessian matrix are

$$\mathbf{H} = \begin{pmatrix} p_{,x^2} & p_{,xy} \\ p_{,xy} & p_{,y^2} \end{pmatrix}, \tag{1}$$

where the second derivatives are given by

$$p_{,x^2} = -\rho\phi_{,x^2t} = \rho k^2\phi_{,t}, \quad p_{,y^2} = -\rho\phi_{,y^2t} = -\rho k^2\phi_{,t}, \quad p_{,xy} = -\rho\phi_{,xyt} \tag{2}$$

It is worth noting that the mean curvature of the pressure (this is also its Laplacian) is zero throughout the fluid. This is not true if the wave is nonlinear. The eigenvalues λ of the matrix $\mathbf{H}$ are determined from

$$\det(\mathbf{H} - \lambda\mathbf{I}) = 0, \quad \Rightarrow \quad \lambda^2 = p_{,xy}^2 - p_{,x^2}p_{,y^2} \tag{3}$$

It is easy to check that the RHS in (3) is positive since $\Delta p = p_{,y^2} + p_{,x^2} = 0$ (true only for linear wave). The eigenvectors $\vec{e}$ follow from the equation $\mathbf{H}\vec{e} = \lambda\vec{e}$, yielding

$$\vec{e} = -p_{,xy}\vec{x} + (p_{,x^2} - \lambda)\vec{y} \tag{4}$$

The eigenvectors can be normalized. It should be noted that their orientation is arbitrary. It is easy to show that the two eigenvectors are orthogonal.

We are interested in the eigenvalue that is positive; it is denoted $\lambda_1 = \sqrt{p_{,xy}^2 - p_{,x^2}p_{,y^2}}$ and its associated eigenvector is $\vec{e}_1 = (e_x, e_y)$. Correspondingly with the nonlinear configuration (see

[1]) we look for the points where the pressure gradient is collinear to the eigenvector $\vec{e}_1$, in other words the points where the following quantity changes sign

$$e_x p_{,y} - e_y p_{,x} = 0 \tag{5}$$

By using (3) and (4), this equation can be turned into

$$p_{,xy}\left(p_{,xy}p_{,y}^2 + 2p_{,x}p_{,y}p_{,x^2} - p_{,xy}p_{,x}^2\right) = 0 \tag{6}$$

In general the term into bracket cannot vanish, it remains $p_{,xy} = 0$. For a monochromatic Airy wave, it is easy to show that the condition $p_{,xy} = 0$ is met beneath the crests and the troughs. In addition the eigenvector cannot be zero, hence $e_y \neq 0$. By using (4) it is obtained $p_{,x^2} < 0$, which means that the free surface elevation $\eta(x,t)$ verifies $\eta_{,x^2} < 0$; consequently this is a crest. We finally check that the two vectors $\vec{e}_1$ and $\vec{\nabla} p$ are collinear, that is to say the following equality is verified

$$|e_x p_{,x} + e_y p_{,y}| = ||\vec{e}_1|| \cdot ||\vec{\nabla} p|| \tag{7}$$

where $e_x = 0$ and $p_{,x} = 0$ along the backbone line. We can conclude, for a monochromatic Airy wave, that the backbone lines are vertical straight lines joining each crest to the bottom. If the water depth is infinite the backbone lines are semi infinite lines. In the developments above, the expression of the velocity potential has not been explicitely required. As a consequence for irregular waves the same conclusion still holds. The analysis exposed in [4] can be revisited. Indeed it is shown how the vertical pressure gradient reaches the Stokes' limit $p_{,y} = -\frac{1}{2}\rho g$ when a crest is close to breaking (see [5]).

The next step is the analysis of true nonlinear wave trains. For that a Boussinesq model (see [3]) yields physically reasonable free surface profiles and the corresponding distributions of velocity potential. Those are used as initial conditions for the numerical code FSID that solves the fully nonlinear free surface boundary conditions in potential theory. The wave trains selected were studied in [2], in particular to produce a focused wave and thus analyze the triggering of the breaking wave. Here we are concerned with a standard wave train well before breaking. The figure below shows the free surface profile at a given instant of the simulation, instant close to the initial time.

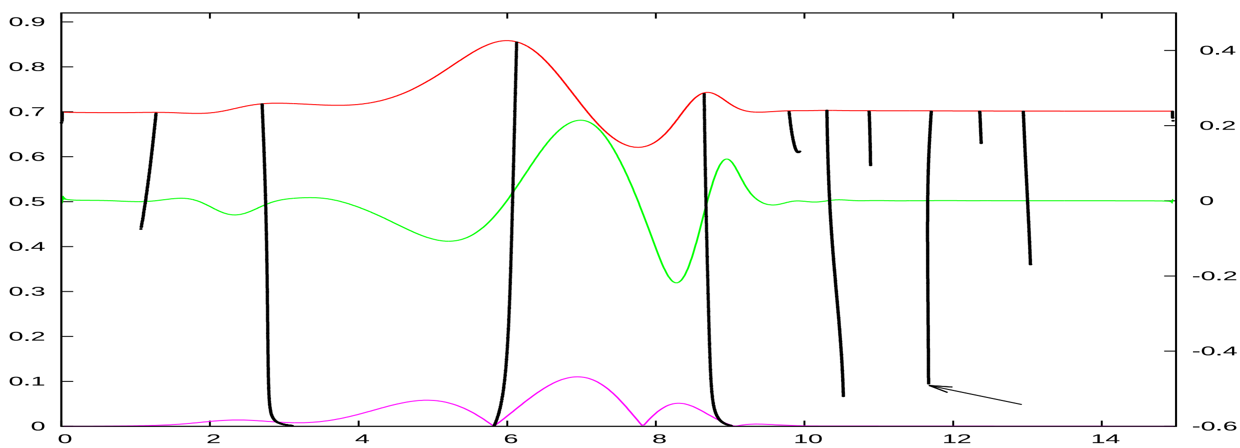

It is observed here that from each of the main crests, emanates a backbone line that reaches the bottom. At these points on the bottom, the horizontal pressure gradient vanishes or changes sign. This characteritics can be used to detect a starting point of the backbone line and then the whole backbone line can be computed iteratively. However, some of the backbone lines stop inside the fluid. That is why the computation of the pressure and its derivatives must be achieved with much accuracy everywhere in the fluid and especially at the free surface. In particular the discrete definition of the free surface must not suffer from pathology like sawtooth instabilities (and the necessary smoothing) that would greatly jeopardize the required accuracy. In that sens the desingularized technique implemented in the present numerical software, allows to reach this accuracy. Indeed the computation of the velocity potential follows from a simple summation of the influence of source singularities located outside the fluide domain. The intensities of these singularities are computed from the Dirichlet condition at the free surface. The temporal and spatial derivatives of the velocity potential are hence computed with the same accuracy than for velocity potential itself. Some care must be only paid to the computation of the time derivative of the intensities of the singularities. The numerical strategy is exposed in [6].

A local analysis of the pressure field at the tip of one of these backbone lines inside the fluid shows that the end point is embedded in a region where the Gaussian curvature changes sign and therefore becomes positive. A closer view of the pressure gradient field is shown below. It corresponds to the tip indicated with an arrow in the first figure above.

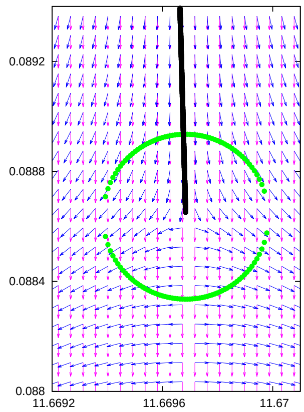

This region surrounding the tip is tiny and roughly circular with diameter about $0.6mm$ to be compared to the water depth $h = 0.7m$. Inside this region, the Gaussian curvature is slightly positive. This means that the two eigenvalues of the Hessian matrix are both negative. As a consequence the shape of the surface made by the pressure (in the coordinate system (x, y) of the plane flow) can be approximated with an elliptic paraboloid which is tangent to the plane that contains the pressure gradient. Two vector fields are superimposed: the pressure gradient and one of the eigenvector of the Hessian matrix. This eigenvector is associated to the eigenvalue that can change sign in the fluid. In the small area under consideration, the pressure gradient is mainly directed vertically downwards. That means that the fluid dynamics is essentially governed by the hydrostatics. However the curvature of the pressure varies locally. Indeed the eigenvector has a discontinuous direction below the tip. Since one of the curvature radius of pressure changes sign along the green line, the pressure is very flat in the closed region. A deeper analysis should provide more insights into this spatial variation. However it is clear that these variations are very weak.

The same simulation leads to a focused wave which does not break. However a slight increase of the initial potential energy (by increasing the initial free surface deformation) would lead to a breaking wave. This has allowed to perform a parametric analysis of the onset of breaking wave (see [7]). Here we consider the state of the focused wave when the main crest reaches its highest amplitude and kinematics. The figure below shows the free surface profile at this precise instant of the simulation.

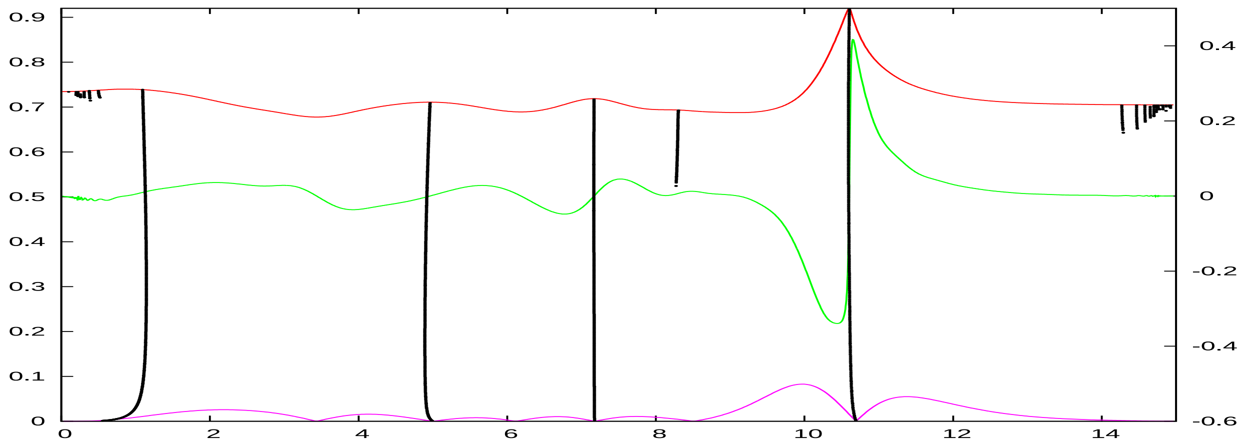

The same characteristics can be observed as before. The main difference with the previous instant concerns the average slope of the backbone line connected to the main crest. Indeed it is now slighly negative. This characterizes a crest which is deccelerating. This is confirmed by examining the spatial variation of the horizontal Lagrangian acceleration at the free surface. This variable is plotted in green in the figure above and its range of variation (divided by the acceleration of gravity) is read on the right vertical axis. It is worth noting at the crest the sharp change of sign of the horizontal acceleration; the fluid deccelerating on the leaside of the wave. This is consistent with the observations of [8] and the fact that the phase speed decreases to a value close to the horizontal fluid velocity (at the crest) which otherwise reaches its maximum value. It is also shown in [7] that along the backbone line linking the bottom to crest, the vertical pressure gradient (made nondimensional with ρg) almost reaches a minimum value $-1/2$ slightly below the crest. This critical threshold also corresponds to the Stokes' limit of 120^o as shown by [5].

3) References

1. Scolan, Y.M., Etienne, S., 2021, Properties of the pressure field in highly nonlinear free surface flows with critical jet. J. Eng Math, 128, 4, doi: 10.1007/s10665-021-10116-4

2. Scolan Y.-M., 2024, On some properties of the pressure in nonlinear two-dimensional potential flow with a free surface, Applied Ocean Research, doi: 10.1016/j.apor.2024.104123.

3. Kimmoun O. and Scolan Y.-M., 2009, Generation of focalized wave packet Proc. 24^{th} International Workshop on Water Waves and Floating Bodies, Zelenogorsk, Russia.

4. Nadaoka, K., Ono, O. and Kurihara, H., 1997, Analysis of near-crest pressure gradient of irregular water waves as a dynamic criterion of breaking, Proc. The Seventh International Offshore and Polar Engineering Conference, Honolulu, Hawaii, USA, May 1997.

5. Longuet-Higgins, M., 1963, The generation of capillary waves by steep gravity waves. Journal of Fluid Mechanics, 16(1), 138-159, doi:10.1017/S0022112063000641

6. Scolan, Y.M., Bingham, H.B., 2024, An analysis of vector and scalar fields in potential free surface flows, Proc. of the 19èmes Journées de l'Hydrodynamique, Nantes - November 2024.

7. Scolan Y.-M. & Etienne S., 2023, Pressure analysis in nonlinear waves by revisiting the breaking wave onset. European Journal of Mechanics / B Fluids 101 (2023), 246–256. 10.1016/j.euromechflu.2023.06.002

8. Banner, M. L., Barthelemy, X., Fedele, F., Allis, M., Benetazzo, A., Dias, F. and Peirson, W. L., 2014, Linking reduced breaking crest speeds to unsteady nonlinear water wave group behavior, Phys Rev Lett., 112.114502.